Gas-Phase Complexes Containing the Uranyl Ion and Acetone

Michael J. Van Stipdonk,* Winnie Chien, Victor Anbalagan, and Kellis Bulleigh

Department of Chemistry, Wichita State University, Wichita, Kansas 67260-0051

Dorothy Hanna

Department of Chemistry, Kansas Wesleyan University, Salina, Kansas 67401

Gary S. Groenewold

Idaho National Engineering and Environmental Laboratory, Idaho Falls, Idaho 83415-2208

Received: July 31, 2004; In Final Form: September 8, 2004

We report here that electrospray ionization (ESI) of uranyl nitrate dissolved in a mixture of H_2O and acetone causes the formation of doubly charged, gas-phase complexes containing UO_2^{2+} "solvated" by neutral ligands. Using mild conditions, the dominant species observed in the ESI mass spectrum contained the uranyl ion coordinated by five acetone ligands, consistent with proposed most-stable structures in the solution phase. However, chemical mass shift data, ion peak shapes, and a plot of fractional ion abundance versus ion desolvation temperature suggest that in the gas phase, and under the ion-trapping and ejection conditions imposed, complexes with five equatorial acetone ligands are less stable than those with four. Multiple-stage tandem mass spectrometry showed that uranyl-acetone complexes dissociate via the elimination of acetone ligands and through pathways that involve reactive collisions with adventitious H_2O in the ion trap. At no point was complete removal of ligands to generate the UO_2^{2+} ion achieved. ESI was also used to generate complex ions of similar composition and ligand number but different charge state for an investigation of the influence of complex charge on the tendency to add ligands by gas-phase association reactions. We found that the addition of a fifth acetone molecule to complexes initially containing four equatorial ligands is more facile for the doubly charged species. The singly charged complex shows a significant back-reaction to eliminate the fifth ligand, suggesting an intrinsic difference in the preferred coordination number for the U(VI) and U(V) complexes in the gas phase.

Introduction

The speciation and reactivity of uranium is a topic of sustained interest because species-dependent chemistry[1] controls processes ranging from nuclear fuel processing[2] to mobility and fate in the geologic subsurface.[3,4] The desire to gain an understanding of intrinsic uranium cation reactivity motivated a wide range of earlier mass spectrometric studies, most focusing on uranium in low-oxidation states (i.e., U^+ and UO^+) and reactions with organic compounds[5−10] or oxidation by small molecules such as O_2, CO, N_2O, and ethylene oxide.[11−14]

Species containing U(IV) and U(VI) are commonly encountered in the environment but have been less extensively studied by mass spectrometry because of a lack of practical means to generate complexes with U in these high-oxidation states. Kemp et al. demonstrated that fast atom bombardment could be used to generate an extensive series of uranium oxo cations, including those with high apparent U oxidation states, from dioxouranium salts.[15] Gresham and co-workers later showed that sputtering of solid UO_3 by energetic ReO_4^- ions could be used to generate sufficient quantities of monopositive uranium oxo cations for investigations of intrinsic hydration rates by ion-trap mass spectrometry (ITMS).[16] More recently, ESI has proven to be an effective tool for generating ions containing U in the higher states and has allowed the investigation of a wide range of uranium species by mass spectrometry and ion mobility mass spectrometry.[17−22] To improve the understanding of intrinsic uranium chemistry, and in particular the chemistry of species in higher oxidation states, we have been studying the species-dependent reactivity of a range of monopositive uranyl-ligand cations using the combination of ESI and ITMS.[22−24] Our focus to date has been on the multiple-stage collision-induced dissociation (CID) of coordinated uranium dioxo cations and on the intrinsic tendency to accept neutral ligands such as H_2O in the gas phase. For example, multiple-stage CID was used to characterize $[UO_2NO_3]^+$, $[UO_2OH]^+$, or $[UO_2OR]^+$ (R = $-CH_3$, $-CH_2CH_3$, and $-CH_2CH_2CH_3$) cations, coordinated by up to three coordinating solvent molecules, that were derived from solutions of uranyl nitrate dissolved in water or mixtures of water and alcohol.[22] Highly coordinated species showed a tendency to eliminate intact coordinating water and alcohol ligands. In contrast, CID of $[UO_2NO_3(ROH)]^+$ eliminated nitric acid to furnish a ligated uranyl-alkoxide cation. For complexes with coordinating water molecules, the multiple-stage CID led to the generation of either $[UO_2OH]^+$ or $[UO_2NO_3]^+$. In another study, we found that the uranyl-2-propoxide monocation, when coordinated by a single 2-propanol molecule, mediated the conversion of the neutral alcohol to acetone and the propoxide ligand to acetaldehyde during the multiple-stage CID experiment.[23]

ESI and multiple-stage CID have also been used to generate bare uranyl hydroxide, nitrate, and acetate monocations for subsequent investigations of intrinsic hydration tendencies.[24] The

* To whom correspondence should be addressed.

10.1021/jp046565p CCC: $27.50
Published on Web 10/30/2004

relative rates for the formation of the monohydrates $[(UO_2A)(H_2O)]^+$, with respect to A (where A = OH, NO_3, or CH_3COO), followed the trend $CH_3COO > NO_3 \gg OH$. The trend was rationalized in terms of the donation of electron density by the strongly basic OH to the uranyl metal center and the reduction of Lewis acidity of U and the presence of increased degrees of freedom to accommodate excess energy from the hydration reaction in CH_3COO and NO_3. The monohydrates also reacted with water, forming dihydrates and then trihydrates. The rates for formation of the nitrate and acetate dihydrates $[(UO_2A)(H_2O)_2]^+$ were very similar to the rates for formation of the monohydrates; the presence of the first H_2O ligand had no influence on the addition of the second. In contrast, formation of the $[(UO_2OH)(H_2O)_2]^+$ was nearly 3 times faster than the formation of the monohydrate.

Gas-phase doubly charged complexes containing the uranyl ion coordinated by neutral ligands have thus far remained elusive and the lack of effective methods for generating such species has impeded characterization of the intrinsic chemistry of the dication and its compounds. In a landmark study, Schwarz and co-workers[12] were able to generate the "bare" uranyl dication by gas-phase oxidation and charge exchange reactions, which yielded a value for the second ionization potential for UO_2 that was consistent with vertical ionization energies that were generated using ab initio calculations. They noted that UO_2^{2+} was thermodynamically stable. As we report here, ESI of uranyl nitrate dissolved in mixtures of H_2O and acetone generates gas-phase complexes containing UO_2^{2+} "solvated" by neutral ligands as well as more conventional monopositive cationic complexes in which, for example, uranyl-nitrate or hydroxide are coordinated by acetone ligands. CID and multiple-stage tandem-ion-trap mass spectrometry were used to elucidate the fragmentation pathways for the various complex ions. Several complex ions were also isolated and stored in the ion trap for varying periods of time to investigate and compare intrinsic ligand (H_2O and acetone) addition reactions.

Experimental Section

ESI-MS, multiple-stage CID, and ion−molecule reactions were carried out using established procedures explicitly described for uranium complexation studies in refs 22 and 24. Uranyl nitrate hexahydrate, $UO_2(NO_3)_2 \cdot 6H_2O$, was purchased from Fluka/Sigma-Aldrich (St. Louis, MO) and used as received. A stock solution of uranyl nitrate solutions (1 mM concentration) was prepared by dissolving the appropriate amount of solid in deionized H_2O. Spray solutions for the ESI experiment were prepared by combining portions of the $UO_2(NO_3)_2 \cdot 6H_2O$ stock solution with acetone such that the composition ranged from 2 to 75% acetone by volume.

ESI mass spectra were collected using a Finnigan LCQ-Deca ion-trap mass spectrometer (ThermoFinnigan Corporation, San Jose, CA). The spray solutions were infused into the ESI-MS instrument using the incorporated syringe pump at a flow rate of 3−5 μL/min. The atmospheric pressure ionization stack settings for the LCQ (lens voltages, quadrupole and octapole voltage offsets, etc.) were optimized for maximum ion transmission to the ion-trap mass analyzer by using the autotune routine within the LCQ Tune program. The spray needle voltage was maintained at +5 kV and the N_2 sheath gas flow at 25 units (arbitrary to the LCQ instrument, corresponding to approximately 0.375 L/min). For most experiments, the heated capillary (used for ion desolvation prior to injection into the ion trap) temperature was maintained between 100° and 120 °C to maximize both the total ion signal and the production of doubly charged complexes. The temperature was ramped in 10° increments during experiments designed to measure the susceptibility of uranyl complexes to undergo thermal dissociation within the heated capillary (vide infra). Helium was used as the bath/buffer gas to improve trapping efficiency and as the collision gas for CID experiments.

For stable gas-phase ions, peak shape profile and chemical mass shift data were collected using the ZoomScan function within the LCQ operating software. The ZoomScan function uses a slower scan-out rate to provide high-resolution mass spectra over a 10 mass unit range, and a previous study by Yost and co-workers[25] demonstrated that general differences in ion stability can be determined using the peak shapes exhibited using this function on the LCQ platform. Chemical mass shifts in ITMS have been discussed in several previous reports.[25−32] The first observations of the shifts (measured ion masses significantly lower than calculated masses for the same species) were attributed to the geometry of the ion trap analyzer, and mass measurement inaccuracies due to geometry have been minimized in commercial ion traps by an increase of the axial dimension of the device.[26,27] Since that time, chemical effects such as polarizability and ion stability have been proposed to account for the persistence of chemical mass shifts in certain experiments.[28−30] Most relevant to the present study, Callahan and co-workers[33] and Yost and co-workers[32] suggested that the tendency for polyatomic species to dissociate during the scan-out period during analytical scans will lead to significant peak fronting/tailing and chemical mass shifts. In our experiments, mass shifts were calculated by subtracting the calculated ion mass (using exact isotope masses) from the measured ion mass.

CID was performed using isolation widths of 2−6 mass units (depending on the species), an activation Q (used to adjust the q_z value for the resonant excitation of the precursor ion during the CID experiment) value of 0.3, activation amplitudes of 10−20% (arbitrary to the LCQ system, represents a percentage of 5 V peak-to-peak normalized for precursor ion mass), and activation times of 30 ms. For intrinsic ligand-addition reaction investigations, all charged species other than the uranyl complex of interest were resonantly ejected from the ion trap. The influence of the q_z setting on the reaction rates for two complex ions, one singly and one doubly charged uranyl-acetone ion, was tested. Through a series of q_z values ranging from 0.09 to 0.6, the difference in measured rates and rate constants was ∼5−10% and within the experimental error typical of the measurements in the ion trap. This observation suggests that the q_z value within this range does not significantly influence the reaction rates for the species reported here and under the reaction conditions employed. This observation is consistent with simulations by Jackson et al which showed little difference in the root-mean-square kinetic energy of U^+ ions in He buffer gas for q_z values of 0.1−0.65 units.[13]

To qualitatively compare the reactivity of the singly and doubly charged species, the complex ions were isolated and stored within the ion trap for times ranging from 1 to 10 000 ms and reacted with neutral reagents (primarily adventitious H_2O along with acetone from the ESI spray solution) within the He bath gas. Following the isolation period, the precursor and product ions were scanned out of the trap and detected as part of the automated mass analysis operation. Reaction sequences and extent of reaction were evaluated by plotting fractional ion abundances versus reaction time. Because neutral concentrations in the electrospray ion-trap experiment are subject to day-to-day variability, kinetic profiles of singly and doubly charged ions were acquired on the same day. The precision of individual

TABLE 1: Mass-to-Charge Ratios, Chemical Composition, and Chemical Mass Shift Values for Uranyl Containing Complex Ions Observed Following ESI of $UO_2(NO_3)_2 \cdot (H_2O)_6$ (1 mM concentration) Dissolved in 40:60 H_2O/Acetone

species	calculated mass	average measured mass	standard deviation (s)	(measured mass − calculated mass)
$[UO_2]^+$	270.041	270.077	0.067	0.036
$[UO_2OH]^+$	287.043	287.093	0.006	0.050
$[UO_2NO_3]^+$	332.028	332.037	0.006	0.008
$[UO_2(acetone)_3(H_2O)]^{2+}$	231.088	230.893	0.023	−0.195
$[UO_2(acetone)_4]^{2+}$	251.104	251.020	0.000	−0.084
$[UO_2(acetone)_5]^{2+}$	280.125	279.940	0.010	−0.185
$[UO_2OH(acetone)_2]^+$	403.127	403.073	0.006	−0.053
$[UO_2OH(acetone)_3]^+$	461.168	460.993	0.006	−0.175
$[UO_2CH_2{=}COCH_3(acetone)_2]^+$	443.158	443.227	0.012	0.069
$[UO_2CH_2{=}COCH_3(acetone)_3]^+$	501.200	501.003	0.012	−0.196
$[UO_2NO_3(acetone)_2]^+$	448.112	448.010	0.000	−0.102
$[UO_2NO_3(acetone)_3]^+$	506.154	505.943	0.006	−0.210
$[acetone + H]^+$	59.050	59.120	0.000	0.070
$[(acetone)_2 + H]^+$	117.091	117.000	0.000	−0.092

ion abundances were about 5−10% (relative standard deviation), and all trends were reproducible over several separate trials.

Results and Discussion

ESI Mass Spectra. The ESI mass spectrum derived from $UO_2(NO_3)_2 \cdot 6H_2O$ dissolved in 40:60 H_2O/acetone, and using a capillary/desolvation temperature of 60 °C, is shown in Figure 1, and the complex ions observed are summarized in Table 1.

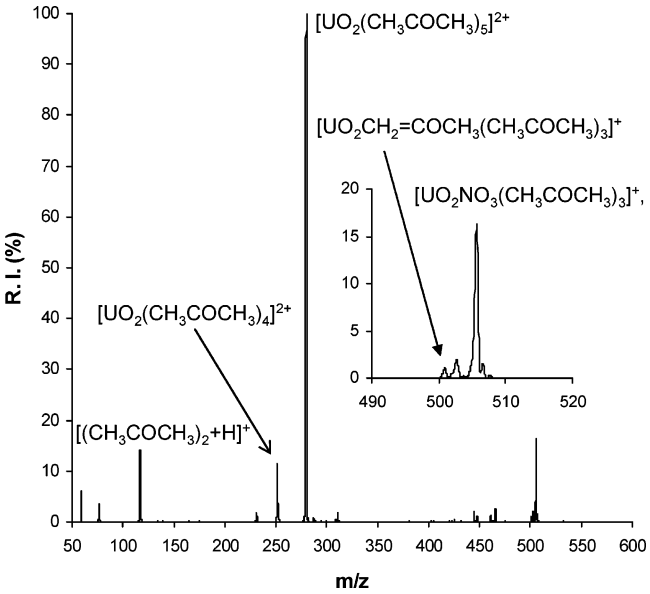

Figure 1. ESI mass spectrum of $UO_2(NO_3)_2 \cdot (H_2O)_6$ (1 mM concentration) dissolved in 50:50 H_2O/acetone. The heated capillary/desolvation temperature was 60 °C. The complexes observed to contain the uranyl ion are listed in Table 1.

The influence of the capillary temperature on the ESI spectrum observed is discussed in a later section. At 60 °C, the principal species observed were $[UO_2(acetone)_4]^{2+}$, $[UO_2(acetone)_5]^{2+}$, and $[UO_2NO_3(acetone)_3]^+$ which appeared in the raw ESI spectrum at mass-to-charge (*m*/*z*) ratios of ∼251, 280, and 506, respectively. ZoomScan, high-resolution mass spectra for these three species, are provided in Figure 2. In the high-resolution mode, the $[UO_2(acetone)_5]^{2+}$ ion (Figure 2b) appeared as a broad peak at *m*/*z* 279.6. The significant tail to the low mass side of the peak is consistent with ion dissociation during the analytical scan out of the ion trap prior to detection. An isotopic peak ∼0.5 mass units (u) higher at ca. *m*/*z* 280.1 (from ^{13}C within the acetone ligands) confirmed a charge state of +2 for the ion. The high-resolution spectrum collected for the $[UO_2(acetone)_4]^{2+}$ ion (Figure 2a) contained peaks at ∼250.9 and 251.43 u (separated by 0.5 u), which confirmed a charge-state assignment

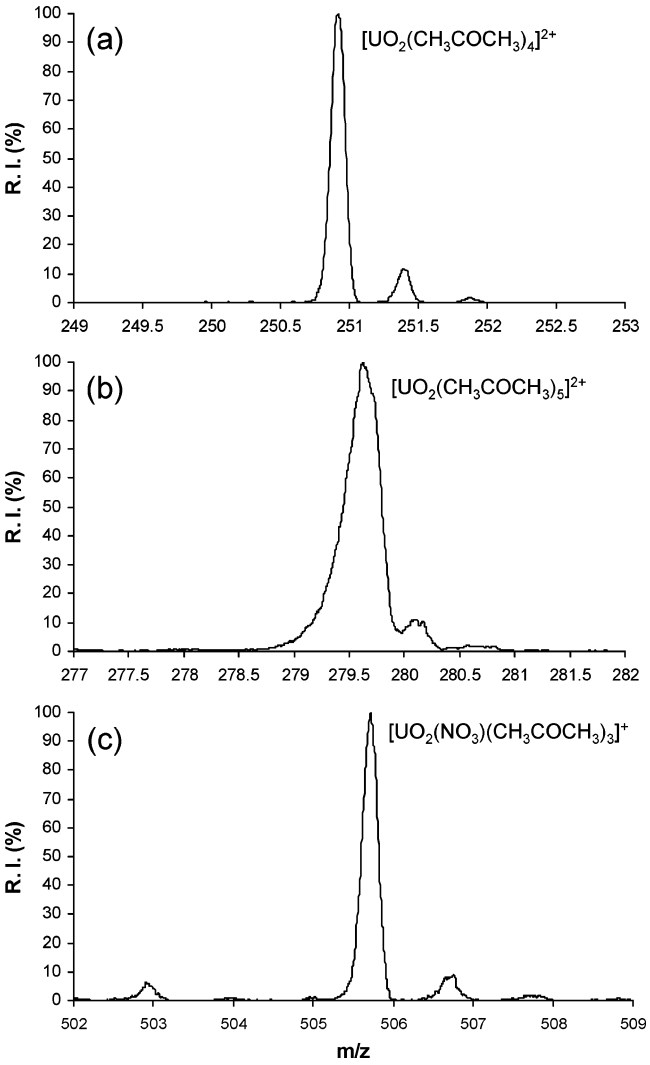

Figure 2. ZoomScan, high-resolution spectra of (a) $[UO_2(acetone)_5]^{2+}$, (b) $[UO_2(acetone)_4]^{2+}$, and (c) $[UO_2NO_3(acetone)_3]^+$.

of +2. In the high-resolution spectrum, the $[UO_2NO_3(acetone)_3]^+$ species appeared as a base peak at *m*/*z* 505.7, with ^{13}C isotopic peak at *m*/*z* 506.7 (1 u higher). We had originally thought that the low abundance ion at *m*/*z* 503 (3 u lower) was due to the ^{235}U isotopic peak, but its abundance is too high for natural U; the ion is probably $[UO_2(CH_3CO_2)(acetone)_3]^+$ which arises

TABLE 2: Peak Width Measurements for Uranyl Containing Complexes Obtained from ZoomScan Spectra

species	average width (10%)	standard deviation (s)	average width (50%)	standard deviation (s)
$[UO_2OH]^+$	0.10	0.00	0.08	0.00
$[UO_2(acetone)_4]^{2+}$	0.20	0.00	0.10	0.00
$[UO_2(acetone)_5]^{2+}$	0.58	0.00	0.28	0.01
$[UO_2OH(acetone)_2]^+$	0.22	0.01	0.11	0.00
$[UO_2OH(acetone)_3]^+$	0.50	0.01	0.26	0.01
$[UO_2CH_2{=}COCH_3(acetone)_2]^+$	0.19	0.01	0.10	0.01
$[UO_2CH_2{=}COCH_3(acetone)_3]^+$	0.43	0.01	0.23	0.01
$[UO_2NO_3(acetone)_2]^+$	0.21	0.01	0.11	0.01
$[UO_2NO_3(acetone)_3]^+$	0.53	0.01	0.27	0.01
$[Acetone + H]^+$	0.19	0.03	0.10	0.00
$[(Acetone)_2 + H]^+$	0.34	0.00	0.17	0.00

from residual acetate that had previously been used in the instrument. The peak spacing for these species confirmed a charge state assignment of +1. Other species of particular interest generated by ESI were those with formula $[UO_2OH(acetone)_3]^+$ at *m*/*z* 461 and $[UO_2CH_2{=}COCH_3(acetone)_3]^+$ at *m*/*z* 501, the latter nominally composed of UO_2^{2+} coordinated by deprotonated acetone and neutral acetone ligands.

$[UO_2(acetone)_4]^{2+}$, $[UO_2(acetone)_5]^{2+}$, and $[UO_2NO_3(acetone)_3]^+$ remained the dominant species as the acetone concentration in the spray solution was decreased to 2% (v:v) (spectra not shown). However, at low acetone concentrations, formation of $[UO_2(acetone)_3(H_2O)]^{2+}$ (*m*/*z* 231) and $[UO_2(acetone)_4]^{2+}$ was favored over $[UO_2(acetone)_5]^{2+}$. The preference for acetone over water as a coordinating ligand in the gas phase constitutes a salient difference in gas-phase uranyl reactivity compared with that in solution, where water is preferred.[34−36] Acetone is a stronger gas-phase nucleophile than is water,[37] which highlights the fact that conditions of aqueous solvation clearly weakens the electron-donating ability of acetone. The formation of doubly charged species is decreased at acetone concentrations greater than 60% (v:v), where the ESI spectrum became dominated by the singly charged species $[UO_2CH_2{=}COCH_3(acetone)_3]^+$ and $[UO_2NO_3(acetone)_3]^+$. The reason for preferential formation of the singly charged species at high acetone concentrations is not known.

Several of the uranyl-containing ions appeared in the ESI specta at *m*/*z* values lower than expected on the basis of calculations from exact isotope masses, even after taking into consideration any uncertainty in measurement accuracy. As noted in the Experimental Section, the degree of peak fronting or tailing and the magnitude of these chemical mass shifts are indicative of ion stability in ion-trap mass spectrometry.[25,32,33] Chemical mass shift data are provided in Table 1 for those uranyl-acetone complex ions that were sufficiently stable to permit collection of ZoomScan high-resolution spectra, and peaks widths for the same ions are shown in Table 2. Peak width data were collected at the 10% peak intensity level (as reported by Yost and co-workers)[25] and at the full width at half-maximum (fwhm). As shown in Table 1, the measured *m*/*z* ratios for protonated acetone (*m*/*z* 59) and $[UO_2OH]^+$ differed from expected, calculated masses by 0.07 and 0.05 u, respectively. Because the measured *m*/*z* values for these two ions were greater than the calculated values and thus not attributable to ion-dissociation process during the high-resolution scans that lead to chemical mass shifts, we chose ±0.07 as a baseline for the mass measurement accuracy in these experiments. Mass differences *beyond* this value were then interpreted as chemical mass shifts due to ion instability.

The data in Table 1 demonstrate that the chemical mass shift increases as the number of coordinating ligands around the uranyl center increases. For example, the calculated chemical mass shifts for $[UO_2(acetone)_4]^{2+}$ and $[UO_2(acetone)_5]^{2+}$ are −0.084 and −0.185 u, respectively. The principal dissociation reaction for $[UO_2(acetone)_5]^{2+}$ involved the elimination of a singly acetone ligand (vide infra); thus, the origin of the large chemical shift for the $[UO_2(acetone)_5]^{2+}$ species was presumably dissociation to produce $[UO_2(acetone)_4]^{2+}$. The increase in shift was not unique to the doubly charged complexes, as the chemical mass shifts for the singly charged, $[UO_2OH]^+$, $[UO_2CH_2{=}COCH_3]^+$, and $[UO_2NO_3]^+$ complexes containing three coordinating acetone ligands were more negative by 0.122, 0.127, and 0.108 u, respectively, when compared to analogous complexes containing only two neutral acetone ligands. As discussed below, the principal dissociation pathways for these species also included the elimination of single coordinating ligands.

As shown in Table 2, trends similar to those for the chemical mass shifts were apparent in the measurements of the peak widths. The peak fronting/tailing was most apparent in the 10% peak width measurement. For example, the peak widths increased from 0.20 u for $[UO_2(acetone)_4]^{2+}$ to 0.58 u for $[UO_2(acetone)_5]^{2+}$ and from 0.21 u for $[UO_2NO_3(acetone)_2]^+$ to 0.53 u for $[UO_2NO_3(acetone)_3]^+$. Regardless of the overall charge state, the chemical mass shift and the degree of peak fronting/tailing was greatest for uranyl complexes with the highest equatorial coordination number. Therefore, the data suggest that the species with high coordination number are the most susceptible to dissociation and least stable. This conclusion is in accord with extensive measurements of alkali- and transition-metal−ligand bond dissociation energies, which in general decrease as the number of ligands increases.[37]

Differences in chemical mass shift and peak width values among complexes of varying size were not unique to those with acetone ligands. For the sake of comparison, Table 3 contains data collected from ZoomScan spectra of uranyl complexes containing acetonitrile ligands. With acetonitrile as cosolvent in the ESI experiment, the major species observed included $[UO_2(acetonitrile)_4]^{2+}$, $[UO_2(acetonitrile)_4(H_2O)]^{2+}$, $[UO_2(acetonitrile)_5]^{2+}$, $[UO_2OH(acetonitrile)_3]^+$, and $[UO_2NO_3(acetonitrile)_3]^+$ (spectrum not shown). The chemical mass shift measured for $[UO_2(acetonitrile)_5]^{2+}$ complex was ca. −0.187, while the shift for the $[UO_2(acetonitrile)_4]^{2+}$ species was +0.147. The shape of the latter complex included a significant tail to the high-mass side, suggesting that the $[UO_2(acetonitrile)_4]^{2+}$ peak may be generated both directly by ESI and by the dissociation of larger complexes such as $[UO_2(acetonitrile)_4(H_2O)]^{2+}$ and $[UO_2(acetonitrile)_5]^{2+}$. The latter process is in effect the opposite to the one that leads to the negative shift values observed for species such as $[UO_2(acetonitrile)_5]^{2+}$ and $[UO_2(acetone)_5]^{2+}$. A positive chemical shift value was also observed for the $[UO_2OH(acetonitrile)_2]^+$ while a large negative value was observed for the $[UO_2OH(acetonitrile)_3]^+$. For the uranyl-nitrate complexes, the $[UO_2OH(acetonitrile)_3]^+$ and $[UO_2OH(acetonitrile)_3]^+$ complexes showed chemical mass shifts of −0.111 and −0.258 u, respectively.

Thermal Dissociation of Complex Ions. The heated capillary of the atmospheric pressure ionization stack on the LCQ platform, used to desolvate ions following ESI and prior to injection into the ion trap, can significantly alter the relative intensity distribution of polyatomic ions observed in ESI mass spectra and has been used as a "thermal reaction vessel" to investigate the thermal dissociation of ions generated by ESI.[38,39] To probe the stability of the uranyl complexes to thermal dissociation prior to injection into the ion trap, ion intensities were measured as a function of capillary temperature. Figure 3

TABLE 3: Chemical Mass Shifts and Peak Width Measurements for Uranyl-Acetonitrile (ACN) Complex Ions

Chemical Mass Shifts				
species	calculated mass	average measured mass	standard deviation (s)	(measured mass − calculated mass)
$[UO_2(ACN)_5]^{2+}$	237.587	237.4	0.021	−0.187
$[UO_2(ACN)_4]^{2+}$	217.073	217.220	0.001	0.147
$[UO_2OH(ACN)_2]^{+}$	369.096	369.120	0.005	0.024
$[UO_2OH(acetone)_3]^{+}$	410.123	409.910	0.007	−0.213
$[UO_2NO_3(acetone)_2]^{+}$	414.081	413.970	0.000	−0.111
$[UO_2NO_3(acetone)_3]^{+}$	455.108	454.850	0.005	−0.258

Peak Widths				
species	average width (10%)	standard deviation (s)	average width (50%)	standard deviation (s)
$[UO_2(ACN)_5]^{2+}$	0.41	0.01	0.2	0.01
$[UO_2(ACN)_4]^{2+}$	0.47	0.01	0.16	0.01
$[UO_2OH(ACN)_2]^{+}$	0.79	0.01	0.32	0.01
$[UO_2OH(acetone)_3]^{+}$	0.49	0.01	0.17	0.01
$[UO_2NO_3(acetone)_2]^{+}$	0.23	0.01	0.13	0.01
$[UO_2NO_3(acetone)_3]^{+}$	0.47	0.01	0.24	0.01

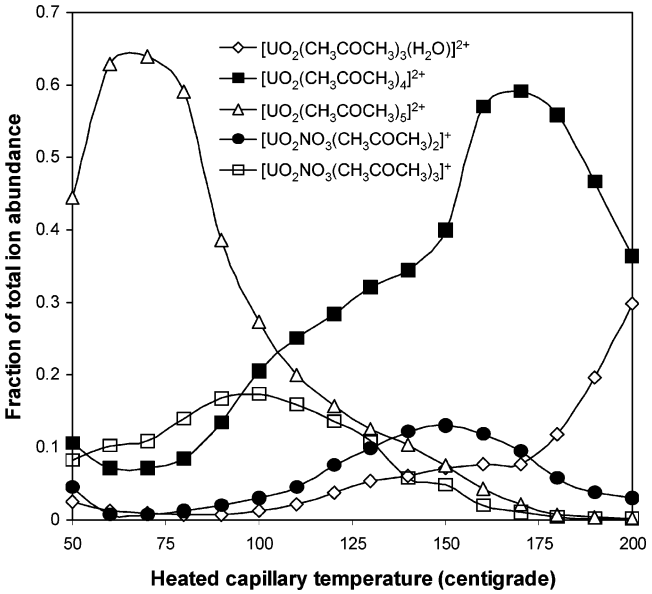

Figure 3. Plot of change in fraction of ion abundance versus heated capillary/desolvation temperature. Complex ions were derived from 1 mM $UO_2(NO_3)_2 \cdot (H_2O)_6$ in 50:50 H_2O/acetone.

shows a plot of the fraction of the total ion abundance for several singly and doubly charged ions plotted versus the temperature of the heated capillary. In the LCQ, the temperature is measured by a thermocouple attached to the capillary and may not accurately reflect the true temperature within the finite space traversed by the ionized species. The plot in Figure 3 should therefore be considered a qualitative measure of the influence of increasing desolvation temperature on relative ion abundance.

At temperatures below 50 °C (data not shown), the ESI spectrum was dominated by the protonated acetone monomer and dimer and protonated clusters of H_2O and acetone. For $[UO_2(acetone)_5]^{2+}$, the fraction of total ion abundance reached a maximum in the range 60−80 °C and decreased as the temperature was raised from 80 to 120 °C. The $[UO_2(acetone)_4]^{2+}$ species exhibited the highest fraction abundance over the range 120−200 °C. At 200 °C, the abundance of $[UO_2(acetone)_4]^{2+}$ was nearly matched by $[UO_2(acetone)_3(H_2O)]^{2+}$. For the singly charged uranyl-containing complexes, the abundance of $[UO_2NO_3(acetone)_3]^{+}$ reached a maximum at ca. 100 °C, then decreased from 100 to 200 °C as the abundance of $[UO_2NO_3(acetone)_2]^{+}$ increased at higher temperatures. Similar profiles were observed for the $[UO_2OH(acetone)_3]^{+}$ and $[UO_2CH_2{=}COCH_3(acetone)_3]^{+}$ species, which were omitted from Figure 3 for the sake of clarity. Beyond 200 °C, the singly charged ions dominated the ESI spectra, and at ca. 250−300 °C only the reduced uranyl ion, UO_2^{+}, and the uranyl hydroxide monopositive cation were observed in high abundance.

In general, similar thermal dissociation profiles were generated for complexes composed of uranyl ion and ligands such as acetophenone and acetonitrile. For the latter case, the complexes proved to be less stable to thermal dissociation than those containing acetone, suggesting stronger uranyl bonds to acetone as compared to acetonitrile. This is consistent with the oxophillic nature of the uranyl ion and preference for coordination by O atoms and with calculations[40] that suggest that the bond distance between a uranyl center and formaldehyde ligands (2.31 Å within a bis-complex) is shorter than for acetonitrile (2.39 Å within an analogous complex).

Using Kohn−Sham density functional theory calculations[40] to treat the hydration of UO_2^{2+}, Spencer et al determined that the most stable equatorial coordination number, n, for the $[UO_2(H_2O)_n]^{2+}$ complexes was 5. By calculating bond-dissociation energies for complexes with varying numbers of H_2O ligands (n), they found the trend to be $\Delta E_{n=5} < \Delta E_{n=6} < \Delta E_{n=4}$. As apparent from Table 1, and as discussed below, a fully hydrated UO_2^{2+} complex ion ($n = 6$) was not observed in the ESI experiment reported here. However, for the uranyl-acetone system, the fact that the $n = 5$ complex decreased and the $n = 4$ increased with increasing desolvation temperature (Figure 3) underscored the susceptibility of $[UO_2(acetone)_5]^{2+}$ to thermal dissociation and clearly showed that the gas-phase complex containing 5 acetone ligands was less stable than one with 4. A recent experimental investigation of UO_2^{2+} in aqueous solution by Neuefeind et al.[41] suggested that there exists in solution a dynamic equilibrium that favors coordination by five H_2O ligands around the equator over 4, but that tetracoordinate species are also present. NMR studies of uncomplexed UO_2^{2+} have been interpreted in terms of five H_2O ligands,[36] although earlier experiments indicated only four.[35] In aggregate, the previously reported extent of complexation in condensed-phase $H_2O-UO_2^{2+}$ complexes was largely consistent with that observed in the present gas-phase uranyl-acetone system.

Accommodation of five acetone ligands around a uranyl center is likely sterically more demanding than the same number of H_2O ligands. A complete analysis of the influence of the

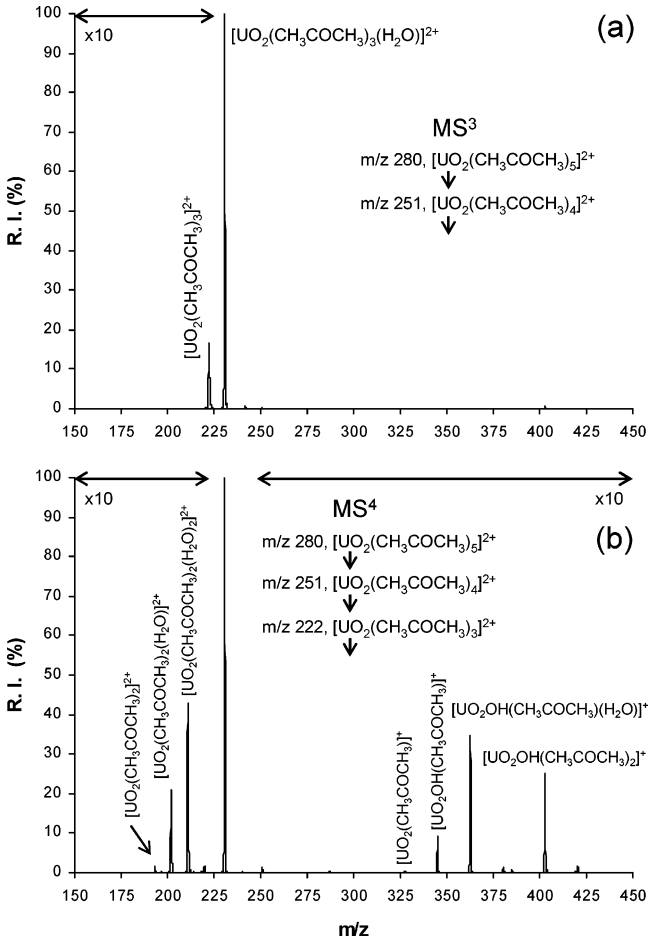

Figure 4. Product ion mass spectra for CID of (a) $[UO_2(acetone)_4]^{2+}$ (MS^3 stage) derived from dissociation of $[UO_2(acetone)_5]^{2+}$ and (b) $[UO_2(acetone)_3]^{2+}$ (MS^4 stage). Product ion compositions are provided in the text.

number and orientation of acetone ligands on the stability and energies of gas-phase complexes will likely require detailed ab initio calculations. To the best of our knowledge, such calculations have not been reported. The comparison of chemical shift and peak width data for complexes containing either acetone or acetonitrile ligands demonstrates that the incorporation of the latter, which would be sterically less demanding for a complex with five ligands, does little to improve the stability of the complex (with the caveat that the bonding interactions between acetonitrile and acetone are likely significantly different). The mass shift and peak shape data, therefore, may point to general differences in gas-phase stability of uranyl-solvent complexes.

Multiple-Stage Tandem Mass Spectrometry. The multiple-stage (MS^n) CID of the major, UO_2 specific complex ions was also investigated. For MS^n of $[UO_2(acetone)_5]^{2+}$, the initial CID stage (MS/MS or MS^2, spectrum not shown) caused the elimination of an acetone ligand to generate $[UO_2(acetone)_4]^{2+}$. The spectrum in Figure 4a shows the result of CID of the $[UO_2(acetone)_4]^{2+}$ product ion (MS/MS/MS or MS^3 stage), which caused the formation of two apparent dissociation product ions: $[UO_2(acetone)_3]^{2+}$ as a minor peak at *m/z* 222 and $[UO_2(acetone)_3(H_2O)]^{2+}$ at *m/z* 231. Subsequent isolation of *only* $[UO_2(acetone)_3]^{2+}$, without imposed collisional excitation, generated $[UO_2(acetone)_3(H_2O)]^{2+}$ in abundance similar to that shown in Figure 4a, indicating that the latter ion is likely generated by rapid hydration of $[UO_2(acetone)_3]^{2+}$ by ion−molecule reactions involving indigenous H_2O in the ion trap. CID of the species at *m/z* 222 in the next dissociation stage (MS^4 stage, Figure 4b) generated $[UO_2(acetone)_2]^{2+}$ as a minor peak at *m/z* 193 and a series of intense hydrated versions of the complex at *m/z* 202 (one H_2O ligand added) and 211 (2 H_2O ligands added). The low abundance of the $[UO_2(acetone)_2]^{2+}$ at the MS^4 stage prohibited further isolation/CID stages. CID of the hydrated species at *m/z* 202 and 211 also failed to produce lower mass, doubly charged products. Rapid reactions with H_2O instead regenerated the hydrates of $[UO_2(acetone)_2]^{2+}$.

Another dissociation pathway observed following the CID of $[UO_2(acetone)_3]^{2+}$ at the MS^4 stage involved formation of product ions with lower charge state (+1). For example, product ions at *m/z* 345, 363, and 403 (Figure 4b) had *m/z* ratios consistent with the formation of $[UO_2OH(acetone)]^+$, $[UO_2OH(acetone)(H_2O)]^+$, and $[UO_2OH(acetone)_2]^+$, respectively. Subsequent CID of $[UO_2OH(acetone)]^+$ and $[UO_2OH(acetone)_2]^+$ (spectra not shown) ultimately led to the production of $[UO_2OH]^+$ at *m/z* 287 by the elimination of neutral acetone ligands. The formation of product ions containing OH, such as $[UO_2OH(acetone)]^+$ and $[UO_2OH(acetone)]^+$, from the doubly charged uranyl-acetone complex presumably involves reactive collisions with H_2O in the ion trap during CID, activation of the H_2O molecule, and retention of hydroxide by the complex. The proposed involvement of H_2O as a collision partner is plausible on the basis of recent work demonstrating that CID within ion-trap instruments involves a significant number of activating collisions between precursor ions and small molecules such as N_2 and H_2O present as contaminants within the He bath gas.[42,43] The formation of a similar activated complex was invoked to explain the formation of a prominent hydrated UO_2^+ ion[22] following the CID of $[UO_2NO_3]^+$ and the generation of $[UO_2OH]^+$ from a uranyl-2-propoxide cation in earlier studies.[23] Assuming the formation of an activated complex including a bound H_2O molecule and retention of OH by the complex (with associated charge reduction), dissociation of the $[UO_2(acetone)_3]^{2+}$ precursor to form $[UO_2OH(acetone)]^+$ and $[UO_2OH(acetone)_2]^+$ might also have produced protonated acetone dimer and monomer, respectively, as complementary product ions. These latter product ions could not be observed during our experiments because of the low-mass cutoff imposed by the q_z value setting used during CID.

CID of the $[UO_2(acetone)_3]^{2+}$ species at the MS^4 stage also generated an ion at *m/z* 328, which is attributed to the formation of a complex containing the uranyl dioxo monocation (UO_2^+) and a single neutral acetone molecule. Subsequent CID of this species caused the elimination of neutral acetone to leave a peak at *m/z* 270. Formation of the reduced uranyl ion at *m/z* 270 was confirmed by a comparison of intrinsic hydration kinetics to previous measured rates for the species[16] (data not shown). At no point during the MS^n dissociation of the doubly charged complex was the bare uranyl ion, UO_2^{2+}, observed. Instead, as described above, the observed tendency was either to generate doubly charged complexes containing a mixture of H_2O and acetone ligands and ultimately undergo charge reduction by charge transfer or acceptance of hydroxide. The reduction in charge state during CID is consistent with both the Lewis acidity of the uranyl ion and fact that the ionization energy of UO_2^+ (ca. 15 eV)[12] is greater than that of either acetone or water (9.7 and 12.6 eV, respectively).[44]

The strong tendency to accept or otherwise interact with H_2O ligands during CID experiments was also apparent during the MS^n dissociation of $[UO_2OH(acetone)_3]^+$, $[UO_2NO_3(acetone)_3]^+$, and $[UO_2CH_2{=}COCH_3(acetone)_3]^+$. For example, CID spectra for the dissociation of $[UO_2NO_3(acetone)_3]^+$ are shown in Figure

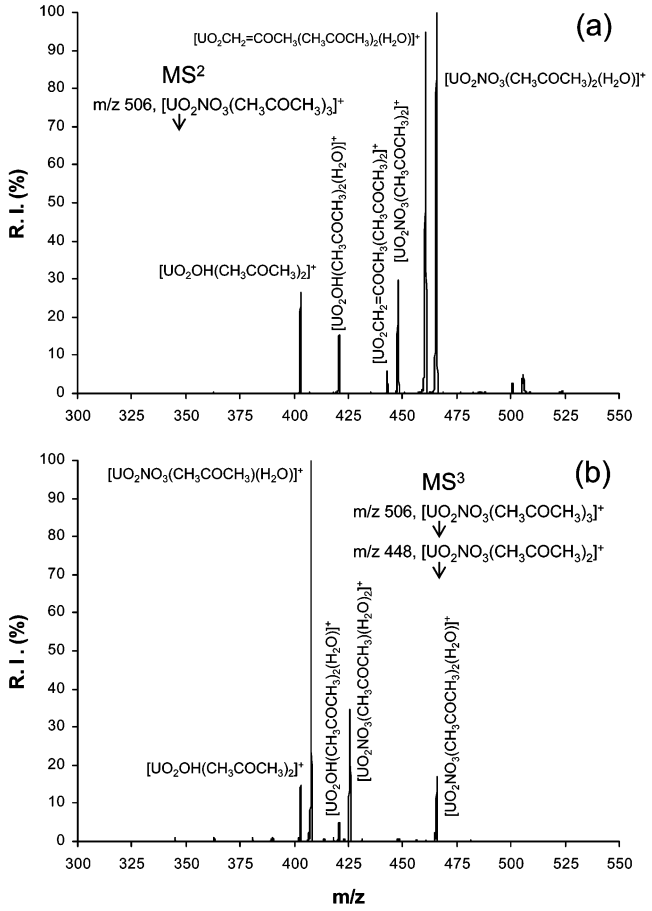

Figure 5. Product ion mass spectra for CID of (a) $[UO_2NO_3(acetone)_3]^+$ (MS/MS or MS^2 stage) and (b) $[UO_2NO_3(acetone)_2]^+$ (MS^3 stage). Product ion compositions are provided in the text.

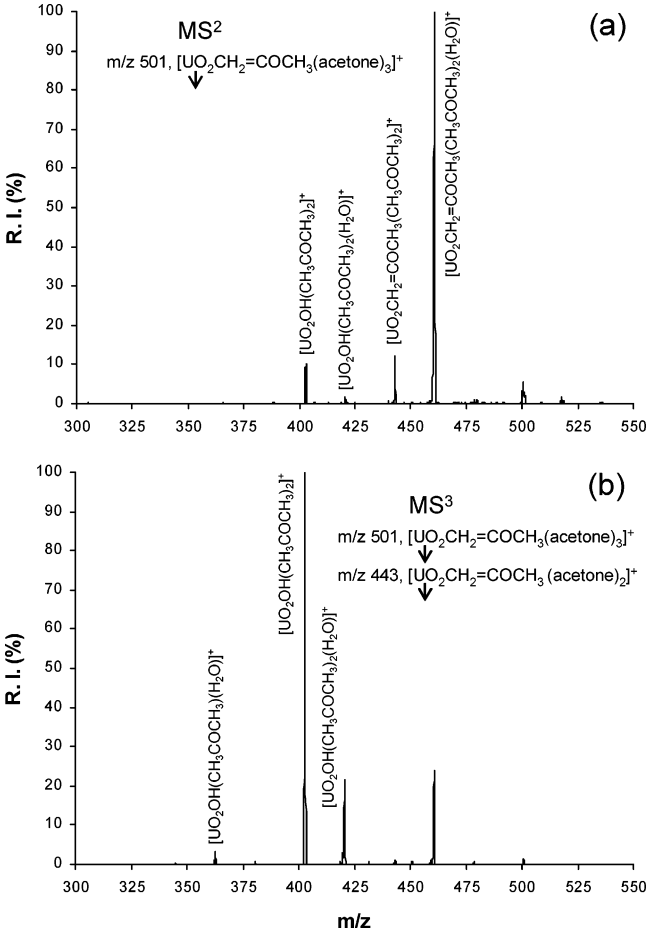

Figure 6. Product ion mass spectra for CID of (a) $[UO_2CH_2{=}COCH_3(acetone)_3]^+$ (MS/MS or MS^2 stage) and (b) $[UO_2CH_2{=}COCH_3(acetone)_2]^+$ (MS^3 stage). Product ion compositions are provided in the text.

5. At the MS/MS stage (Figure 5a), CID lead to three pathways that included (a) the elimination of an acetone ligand to form $[UO_2NO_3(acetone)_2]^+$ at *m*/*z* 448, (b) the elimination of HNO_3 (*m*/*z* 443, discussed below), and (c) the formation of $[UO_2OH(acetone)_2]^+$ at *m*/*z* 403: all three product ions appeared as minor peaks in the CID spectrum. The most abundant apparent products observed were instead hydrated (one additional H_2O ligand added) versions of the product ions at *m*/*z* 443 and 448. The $[UO_2OH(acetone)_2]^+$ ion was the principal dissociation product for the CID of $[UO_2OH(acetone)_3]^+$ (spectrum not shown), and the MS^n dissociation pathways were the same for both the nitrate and hydroxide precursor species. Subsequent CID of the $[UO_2NO_3(acetone)_2]^+$ species at *m*/*z* 448 (Figure 5b) caused the formation of $[UO_2OH(acetone)_2]^+$, $[UO_2NO_3(acetone)(H_2O)]^+$, $[UO_2OH(acetone)_2(H_2O)]^+$, and $[UO_2NO_3(acetone)(H_2O)_2]^+$ at *m*/*z* 403, 408, 421, and 426, respectively.

At the MS/MS stage, elimination of HNO_3 from $[UO_2NO_3(acetone)_3]^+$ generated a product ion at *m*/*z* 443, consistent with a species with formula $[UO_2CH_2{=}COCH_3(acetone)_2]^+$. The same product was observed following the CID (MS/MS) of $[UO_2CH_2{=}COCH_3(acetone)_3]^+$ (Figure 6a). The appearance of the species during the CID of $[UO_2NO_3(acetone)_3]^+$ suggests the proton transfer occurs, via keto−enol tautomerism, from an acetone ligand to NO_3, with subsequent elimination of neutral nitric acid. Deuterium labeled (d_6) acetone was used to generate $[UO_2NO_3(d_6\text{-acetone})_3]^+$. CID of this species (spectrum not shown) caused only the elimination of neutral deuterium labeled acetone ligand, with no observed loss of DNO_3 or HNO_3. However, the lack of a pathway involving the elimination of DNO_3 does not necessarily rule out a mechanism in which a proton was transferred from the protium form of acetone to nitrate: a kinetic isotope effect may alter the tendency for H/D transfer in the CID reaction and the probability for observing the reaction when using the deuterium labeled form of the complex, and the low abundance of *m*/*z* 443 may make observation of a low abundance fragmentation difficult. A mechanism for the elimination of HNO_3 that involves a reactive collision with gas-phase H_2O molecule cannot explain the *m*/*z* value of the product ion, which clearly indicated the presence of a deprotonated acetone ligand.

As noted earlier, CID (MS/MS, Figure 6a) of $[UO_2CH_2{=}COCH_3(acetone)_3]^+$ generated $[UO_2CH_2{=}COCH_3(acetone)_2]^+$ at *m*/*z* 443, a hydrated form of the complex, $[UO_2CH_2{=}COCH_3(acetone)_2(H_2O)]^+$ at *m*/*z* 461, and a product ion at *m*/*z* 403. The peak at *m*/*z* 403 was the major species formed following subsequent CID of $[UO_2CH_2{=}COCH_3(acetone)_2]^+$ (MS^3, Figure 6b), along with peaks at *m*/*z* 363 and 421, consistent with the formation of $[UO_2OH(acetone)_2]^+$, $[UO_2OH(acetone)(H_2O)]^+$, and $[UO_2OH(acetone)_2(H_2O)]^+$, respectively. The assignment of composition as acetone/H_2O ligated uranyl-hydroxide cation was based on the observation that the subsequent CID of these species generated CID spectra that were very similar to those for product ions generated instead from the MS^n of $[UO_2OH(acetone)_3]^+$, that is, directly from a uranyl-hydroxide based complex.

Gas-Phase Ligand Addition Reactions. The general tendency for several uranium-acetone complexes to accept addition ligands via gas-phase association reaction was probed by

selective isolation and storage of the species in the ion trap without imposed collisional activation. Our previous investigation of the intrinsic tendency for monopositive uranyl-ligand cations (uranyl hydroxide, nitrate, and acetate) demonstrated that the maximum number of H_2O molecules added, regardless of the species isolated, was three.[16,22] For the uranyl-hydroxide species in particular, the lack of a fourth H_2O molecule suggested a preferred gas-phase equatorial coordination number of 4 (three H_2O molecules and the OH ligand). Subsequent investigations of the intrinsic hydration of uranyl alkoxides also showed the uptake of a maximum of three H_2O molecules. However, each of the species studied in the earlier investigations was a monopositive cation, and conclusive statements about the intrinsic tendency for true uranyl complexes to hydrate or otherwise participate in ion−molecule reactions require a clear understanding of the influence of charge state on reaction rates and preferred coordination number. The species at *m*/*z* 501 generated by ESI, $[UO_2CH_2{=}COCH_3(acetone)_3]^+$, contains one less proton than the doubly charged ion at *m*/*z* 251, $[UO_2(acetone)_4]^{2+}$, but maintains an equal number of coordinating ligands around the UO_2 core. The lack of a proton causes the overall charge of the former complex to be lower than the latter. This fact allowed us to isolate and store in the ion trap species of nearly identical mass (and presumably conformation) but with different charge state to probe the influence of the latter parameter on the intrinsic tendency to accept ligands by gas-phase association reactions. Figure 7 shows the results of isolating the two species in the ion trap for periods ranging from 1 ms to 10 s. During the imposed isolation period, the species were exposed to H_2O and acetone within the He buffer gas. It was assumed in the experiments that coordination of the uranyl ion by the deprotonated acetone ligand occurs through the O atom and that the overall coordination structure is similar for the two species. As noted in the Experimental Section, the reaction rates for both species did not change significantly with changes in the q_z value during the isolation experiments.

In the present case, despite the high H_2O concentration in the ion trap, the doubly charged species showed a very low tendency to hydrate. Instead, the species reacted nearly to completion by adding a fifth acetone ligand. In contrast to this behavior, the singly charged species showed a greater tendency to hydrate, rapidly exchanging the H_2O ligand for acetone.[16]

As shown in Figure 7, both species showed a tendency to undergo ligand addition reactions. The results from a direct comparison of the doubly and singly charged UO_2-acetone complexes demonstrate significantly higher reaction tendencies for the former over the latter. Our previous experiments have established that the amount of adventitious H_2O in the ion trap is significantly (2−3 times) greater that neutral "reagent" admitted via its use as a component of the spray solvent.[45] The doubly charged species prefers to accept only the more basic acetone molecule, despite the high H_2O concentration in the ion trap, while the singly charged species shows a significant tendency to hydrate at short reaction times, rapidly exchanging the hydrated water for acetone. This appears to be the primary mode of acetone addition at short isolation times for this species. However, the singly charged species came to an apparent equilibrium with respect to acetone addition, which we interpret as reflecting a significant reverse reaction that is actually the collisionally assisted elimination of the fourth acetone ligand. Apparent reverse reactions have proven to be necessary in several earlier investigations of intrinsic hydration rates.

Full kinetic modeling of the ligand addition reactions is currently underway and will be reported in detail in a future publication. Preliminary kinetic modeling suggests that the reactions for the doubly charged complex include the (slow) direct addition of H_2O, exchange of H_2O for acetone, and direct addition of acetone. For the singly charged species, the modeling suggests that the reactions include the direct addition of H_2O and the exchange of bound H_2O for acetone. The modeling for this species also requires the inclusion of a significant back reaction involving the elimination of acetone. After long periods of isolation in the ion trap (>1000 ms), modeling of kinetic profiles obtained from the experimental data suggests a significant decrease in the reactivity of the precursor species for $[UO_2(CH_2{=}CHOCH_3)(acetone)_3]^{+1}$ and, to a much lesser degree, for $[UO_2(NO_3)(acetone)_2]^+$ suggesting that ligand reorganization or rearrangement may be occurring. This apparent change in kinetic behavior was experimentally verified for $[UO_2(CH_2{=}COCH_3)(acetone)_3]^{+1}$, for which the fractional abundance of parent species remaining at isolation times greater than 4000 ms was great enough to allow re-isolation of the unreacted complex. Structural analyses of the most probable conformations for the singly charged uranyl-acetone complex, $[UO_2CH_2{=}COCH_3(acetone)_3]^+$, and the doubly charged analogue are currently underway using density functional theory calculations.

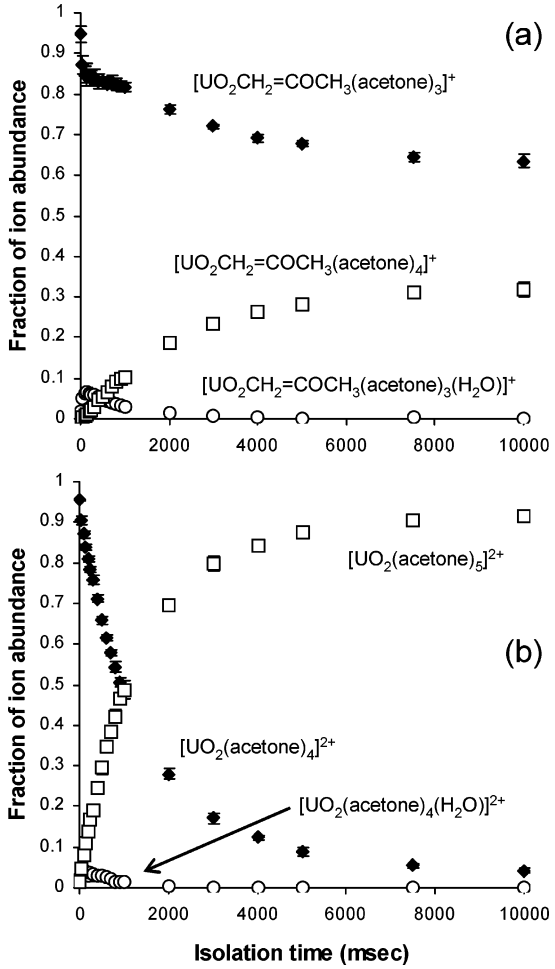

Figure 7. Plot of change in fraction of total ion abundance versus isolation time for storage of (a) $[UO_2CH_2{=}COCH_3(acetone)_3]^+$ and (b) $[UO_2(acetone)_4]^{2+}$ in the ion trap, without imposed collisional activation. Species were exposed to similar environments of H_2O and acetone in He.

Figure 8 shows the reaction kinetics profiles for $[UO_2OH(acetone)_2]^+$, $[UO_2CH_2{=}COCH_3(acetone)_2]^+$, and $[UO_2NO_2(acetone)_2]^+$. Each species was isolated directly from the ESI spectrum, though each could also be generated using a single

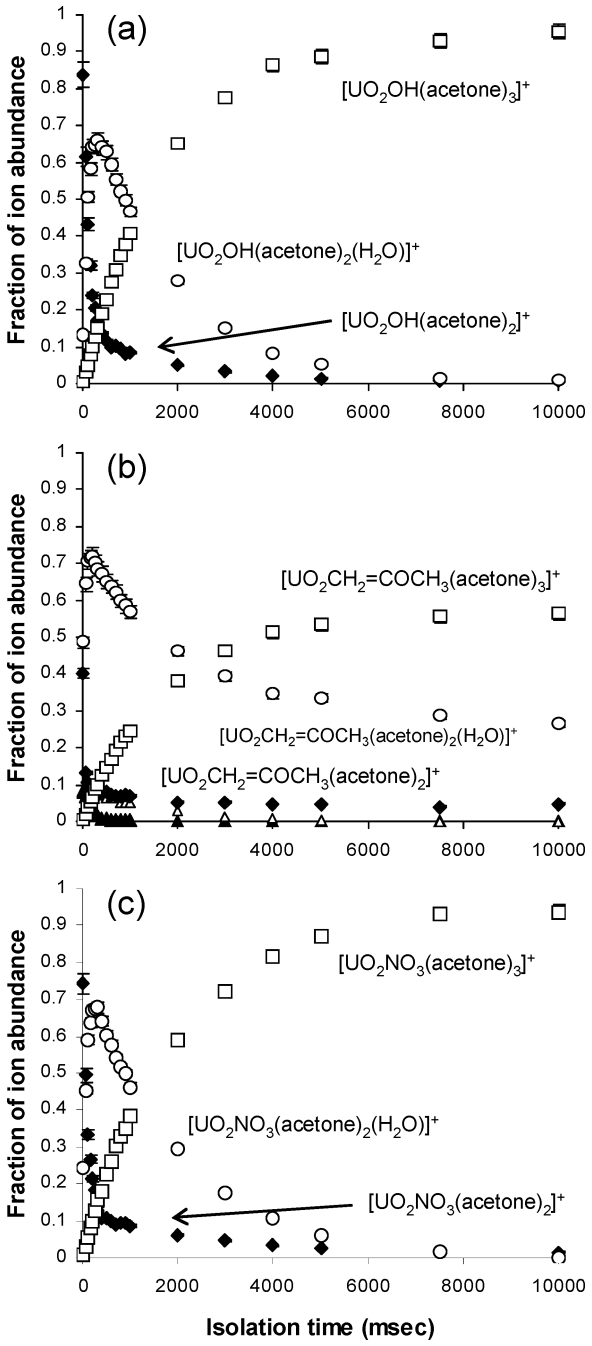

Figure 8. Plot of change in fraction of total ion abundance versus isolation time for storage of (a) $[UO_2OH(acetone)_2]^+$, $[UO_2CH_2{=}COCH_3(acetone)_2]^+$, and (c) $[UO_2NO_3(acetone)_2]^+$ in the ion trap, without imposed collisional activation. Species were exposed to similar environments of H_2O and acetone in He.

CID stage from fully coordinated precursors. The "undercoordinated" complexes showed a greater tendency to accept H_2O ligands at earlier stages than to the more coordinatively saturated $[UO_2CH_2{=}COCH_3(acetone)_3]^+$ and $[UO_2(acetone)_4]$ species.

Conclusions

We have used ESI to generate series of singly and, more importantly, doubly charged complex ions containing UO_2 and acetone ligands. The most abundant ion generated by ESI under low-energy desolvation conditions is the doubly charged $[UO_2(acetone)_5]^{2+}$, a species containing the preferred number of equatorial coordinating ligands as suggested by condensed-phase and theoretical investigations. Chemical mass shifts and thermal dissociation data suggest that the elimination of one acetone ligand from the $[UO_2(acetone)_5]^{2+}$ species can be accomplished with only modest increases in energy; however, the resulting $[UO_2(acetone)_4]^{2+}$ will readily add the ligand back, underscoring the stability of the pentacoordinated UO_2^{2+} complex. The influence of the +2 charge can be qualitatively assessed by a comparison with the singly charged $[UO_2(CH_2{=}COCH_3)(acetone)_3]^+$: this ion will also add a fifth equatorial acetone ligand, but in the ion trap the reaction never proceeds to completion, and the apparent equilibrium favors the tetracoordinated, singly charged UO_2 complex.

Multiple-stage CID demonstrated that the doubly charged species is reluctant to shed its full complement of coordinating ligands, preferring instead to generate hydrated product ions (H_2O replacing acetone ligands eliminated in the CID reactions) or undergo charge reduction reactions to cations such as $[UO_2OH]^+$ and UO_2^+ coordinated by acetone or H_2O. In contrast, elimination of all coordinating neutral ligands can be achieved in CID of singly charged complexes. Gas-phase ion molecule reactions involving $[UO_2CH_2{=}COCH_3(acetone)_3]^+$ and $[UO_2(acetone)_4]^+$ demonstrate that the singly charged species has a lower tendency to undergo ligand addition reactions compared with the doubly charged species.

The production of doubly charged complexes is not limited to the use of acetone or acetonitrile cosolvent as demonstrated in this report. Preliminary studies indicate that true uranyl complexes can be created by ESI when 2- or 3-pentanone, acetophenone, tetrahydrofuran, dimethyl sulfoxide, or nitrobenzene are used in place of acetone. Efforts to generate doubly charged, hydrated uranyl complexes have failed, even when using salts of the uranyl ion with weakly coordinating anions such as perchlorate. As demonstrated in earlier studies, in aqueous solution devoid of a strongly coordinating ligand such as acetone, the ESI spectrum is dominated by $[UO_2A]^+$, where A is, for example, OH or NO_3, coordinated by solvent molecules.

Acknowledgment. MVS acknowledges support for this work by a grant from the National Science Foundation (CAREER-0239800), a First Award from the Kansas Technology Enterprise Corporation/Kansas NSF EPSCoR program, and a subcontract from the U.S. Department of Energy through the INEEL Institute. D.H. acknowledges the support of the Wichita State University Research Sites for Educators in Chemistry program sponsored by the National Science Foundation. G.S.G. acknowledges support by the U.S. Department of Energy, Environmental Systems Research Program, under contract DE-AC-07-99ID13727. Funds for the purchase of the LCQ-Deca instrument were provided by the Kansas NSF EPSCoR program and the Wichita State University College of Liberal Arts and Sciences.

References and Notes

(1) Weigel, F. Uranium. In *The Chemistry of the Actinide Elements*; Katz, J. J., Morss, L. R., Seaborg, G. T., Eds.; Chapman and Hall: London, 1986; p 169.

(2) Greenwood, N. N.; Earnshaw, A. *Chemistry of the Elements*; Butterworth Heinemann: Oxford, U.K., 1997.

(3) Murphy, W. M.; Shock, E. L. Environmental Aqueous Geochemistry of Actinides. In *Uranium: Mineralogy, Geochemistry and the Environment*; Burns, P. C., Finch, R., Eds.; Mineralogical Society of America: Washington, DC, 1999; p 221.

(4) Brookins, D. G. *Geochemical Aspects of Radioactive Waste Disposal*; Springer-Verlag: New York, 1984.

(5) Gibson, J. K. *Int. J. Mass Spectrom. Ion Processes* **2002**, *213*, 1.

(6) Heinemann, C.; Cornehl, H. H.; Schwarz, H. *J. Organomet. Chem.* **1995**, *501*, 201−209.

(7) Gibson, J. K. *Organometallics* **1997**, *16*, 4214−4222.

(8) Gibson, J. K. *J. Am. Chem. Soc.* **1998**, *120*, 2633−2640.

(9) Gibson, J. K. *J. Mass Spectrom.* **1999**, *34*, 1166−1177.
(10) Gibson, J. K. *J. Vac. Sci. Technol., A-Vac. Surf. Films* **1997**, *15*, 2107−2118.
(11) Armentrout, P. B.; Beauchamp, J. L. *Chem. Phys.* **1980**, *50*, 27−36.
(12) Cornehl, H. H.; Heinemann, C.; Marcalo, J.; deMatos, A. P.; Schwarz, H. *Angew. Chem., Int. Ed. Engl.* **1996**, *35*, 891−894.
(13) Jackson, G. P.; King, F. L.; Goeringer, D. E.; Duckworth, D. C. *J. Phys. Chem. A* **2002**, *106*, 7788−7794.
(14) Gibson, J. K. *J. Mass Spectrom.* **2001**, *36*, 284−293.
(15) Kemp, T. J.; Jennings, K. R.; Read, P. A. *J. Chem. Soc., Dalton Trans.* **1995**, 885−889.
(16) Gresham, G. L.; Gianotto, A. K.; Harrington, P. de B.; Cao, L.; Scott, J. R.; Olson, J. E.; Appelhans, A. D.; Van Stipdonk, M. J.; Groenewold, G. S. *J. Phys. Chem. A* **2003**, *107*, 8530−8538.
(17) Moulin, C.; Charron, N.; Plancque, G.; Virelizier, H. *Appl. Spectrosc.* **2000**, *54*, 843−8.
(18) Wu, Q. C. X.; Hofstadler, S. A.; Smith, R. D. *J. Mass Spectrom.* **1996**, *31*, 669−675.
(19) Dion, H. M.; Ackerman, L. K.; Hill, H. H. *Talanta* **2002**, *57*, 1161−1171.
(20) Dion, H. M. A.; Ackerman, L. K.; Hill, H. H. *Int. J. Ion Mobil. Spectrom.* **2001**, *4*, 31−33.
(21) Pasilis, S. P.; Pemberton, J. E. *Inorg. Chem.* **2003**, *42*, 6793−6800.
(22) Van Stipdonk, M.; Anbalagan, V.; Chien, W.; Gresham, G.; Groenewold, G.; Hanna, D. *J. Am. Soc. Mass Spectrom.* **2003**, *14*, 1205−1214.
(23) Van Stipdonk, M. J.; Chien, W.; Anbalagan, V.; Gresham, G.; Groenewold, G. S. *Int. J. Mass Spectrom.* **2004**, in press.
(24) Chien, W., Anbalagan, V.; Zandler, M.; Van Stipdonk, M.; Hanna, D.; Gresham, G.; Groenewold, G. *J. Am. Soc. Mass Spectrom.* **2004**, *15*, 777−783.
(25) McClellan, J. E.; Murphy, J. P., III; Mulholland, J. J.; Yost, R. A. *Anal. Chem.* **2002**, *74*, 402−412.
(26) Wells, J. M.; Plass, W. R.; Patterson, G. E.; Ouyang, Z.; Badman, E. R.; Cooks, R. G. *Anal. Chem.* **1999**, *71*, 3405−3415.
(27) Gill, L. A.; Wells, Amy, J. W.; Vaughn, W. E.; Cooks, R. G. *Int. J. Mass Spectrom.* **1999**, *188*, 87−93.
(28) Bortolini, O.; Spalluto, G.; Traldi, P. *Org. Mass Spectrom.* **1994**, *29*, 269.
(29) Traldi, P.; Favretto, D.; Catinella, S.; Bortolini, O. *Org. Mass Spectrom.* **1993**, *28*, 745.
(30) Bortolini, O.; Catinella, S.; Traldi, P. *Org. Mass Spectrom.* **1992**, *27*, 927.
(31) Peng, Y.; Plass, W. R.; Cooks, R. G. *J. Am. Soc. Mass Spectrom.* **2002**, *13*, 623−629.
(32) Murphy, J. P., III; Yost, R. A. *Rapid Commun. Mass Spectrom.* **2000**, *14*, 270−273.
(33) Vachet, R. W.; Hartmann, J. A. R.; Callahan, J. H. *J. Mass Spectrom.* **1998**, *33*, 1209−1225.
(34) Burgess, J. *Metal Ions in Solution*; 1978; p 169.
(35) Fratiello, A.; Kubo, V.; Lee, R. E.; Schuster, R. E. *J. Phys. Chem.* **1970**, *74*, 3726−3730.
(36) Bardin, N.; Rubini, P.; Madic, C. *Radiochim. Acta* **1998**, *83*, 189−194.
(37) Rodgers, M. T.; Armentrout, P. B. *Mass Spectrom. Rev.* **2000**, *19*, 215−247.
(38) Busman, M.; Rockwook, A. L.; Smith, R. D. *J. Phys. Chem.* **1992**, *96*, 2397.
(39) Van Stipdonk, M. J.; Ince, M. P.; Perera, B. A.; Martin, J. A. *Rapid Commun. Mass Spectrom.* **2002**, *16*, 355−363.
(40) Spencer, S.; Gagliardi, L.; Handy, N. C.; Ioannou, A. G.; Skylaris, C.-K.; Willets, A.; Simper, A. M. *J. Phys. Chem. A* **1999**, *103*, 1831−1837.
(41) Neuefeind, J.; Soderholm, L.; Skanthakumar, S. *J. Phys. Chem. A* **2004**, *108*, 2733−2739.
(42) Catinella, S.; Pelizzi, N.; Barboso, S.; Favretto, D.; Seraglia, R.; Traldi, P. *Rapid Commun. Mass Spectrom.* **2002**, *16*, 1897−1902.
(43) Goeringer, D. E.; Duckworth, D. C.; McLuckey, S. A. *J. Phys. Chem. A* **2001**, *105*, 1882−1889.
(44) Rosenstock, H. M.; Draxl, K.; Steiner, B. W.; Herron, J. T. *J. Phys. Chem. Ref. Data* **1977**, *6* (Suppl. 1), 783.
(45) Hanna, D.; Silva, M.; Morrison, J.; Tekarli, S.; Anbalagan V.; Van Stipdonk, M. *J. Phys. Chem. A* **2003**, *107*, 5528−5537.